Management of Biological Invasions (2014) Volume 5, Issue 1: 39–54
doi: http://dx.doi.org/10.3391/mbi.2014.5.1.04

Open Access

Research Article

Mathematical model describing the population dynamics of *Ciona intestinalis*, a biofouling tunicate on mussel farms in Prince Edward Island, Canada

Thitiwan Patanasatienkul*, Crawford W. Revie, Jeff Davidson and Javier Sanchez

Department of Health Management, Atlantic Veterinary College, University of Prince Edward Island, 550 University Avenue, Charlottetown, PE, Canada, C1A 4P3

E-mail: thitiwan.patanasatienkul@gmail.com (TP), crawfordrevie@gmail.com (CR), davidson@upei.ca (JD), jsanchez@upei.ca (JS)

**Corresponding author*

Received: 7 August 2013 / Accepted: 16 December 2013 / Published online: 1 February 2014

Handling editor: Richard Piola

Abstract

A mathematical model was used to describe the population of the aquatic invasive species, *Ciona intestinalis* in the presence of cultured mussel production. A differential equation model was developed to represent the key life stages: egg, larva, recruit, juvenile and adult. Stage transition rates were calculated from time spent in a stage and transition probabilities. Because surface availability for the settlement phase is a key determinant of population growth, dead juvenile and dead adult stages were also modelled, together with their drop-off rates. This model incorporated temperature dependencies and an environmental carrying capacity. Model validation was carried out against field data collected from Georgetown Harbour, in 2008. Relative sensitivity indices were calculated to determine the most influential factors in the model. The results indicated that the modelled outputs were broadly in agreement with the observed data. Under baseline conditions the number of *C. intestinalis* increased from early September to late October, after which they reached a plateau at an abundance of approximately five individuals per cm^2. Sensitivity analyses revealed that a reduction in spawning interval or the development time of larva accelerated *C. intestinalis* population growth. In contrast, decreasing either carrying capacity or the percentage drop-off of live juvenile and adult stages resulted in a decline in the population. This research provides the first detailed model describing population dynamics of *C. intestinalis* in mussel farms and will be valuable in exploring effective treatment strategies for this invasive species.

Key words: mathematical model, population dynamics, *Ciona intestinalis*, aquatic invasive species, tunicates, blue mussel

Introduction

Mussels accounted for 66% of total Canadian shellfish production (38,646 tonnes), with an estimated market value of CAD$39 million, in 2011 (Statistics Canada 2012). The Prince Edward Island (PEI) blue mussel (*Mytilus edulis* Linnaeus, 1758) industry produces approximately 80% of all mussels cultured in Canada (Statistics Canada 2012). Over the past 15 years the industry has encountered increasing challenges related to aquatic invasive species, especially tunicates. These biofouling species compete for food and space, reducing water flow rates from the species overgrowth, jeopardizing mussel health and yield, which can cause significant economic losses to mussel farmers and processors as a result of the costs associated with controlling their population growth as well as the additional labour costs during the mussel cleaning process at processing plants (Carver et al. 2006; Locke et al. 2009). Four species of invasive tunicates are found in PEI (Fisheries and Oceans Canada 2006; Macnair 2005): clubbed tunicate (*Styela clava* Herdman, 1881), vase tunicate (*Ciona intestinalis* Linnaeus, 1767), golden star tunicate (*Botryllus schlosseri* Pallas, 1766), and violet tunicate (*Botrylloides violaceus* Oka, 1927). Of these, the vase tunicate is considered to be the greatest threat for PEI aquaculture. Two years after the first identification of *C. intestinalis* in Montague River, PEI in the autumn of 2004, it became a dominant fouling species, causing severe problems for the PEI mussel industry (Carver et al. 2006; Ramsay et al. 2008).

C. intestinalis is a solitary tunicate, with a short-lived planktonic stage before settling on a suitable substrate during metamorphosis and becoming a sessile filter feeder (Carver et al. 2006). The growth and reproductive rates are strongly temperature dependent (Dybern 1965; Carver et al. 2006); exhibiting rapid growth in the summer, before decreasing with declining temperature (Carver et al. 2006). A study of *C. intestinalis* populations in Atlantic coast of Nova Scotia, Canada estimated 12,000 eggs were produced per a 100-mm long individual over a season (Carver et al. 2003). Another study in Japan gave an estimate of 100,000 eggs per individual (Yamaguchi 1975). With its high fecundity and ability to reproduce rapidly (Carver et al. 2006), a mussel sock can be covered with *C. intestinalis* individuals in a short time; increasing the biomass on the mussel socks and resulting in mussel mortality through fall-off. To mitigate this, farmers remove tunicates from mussel socks by chemical and mechanical methods including 4% acetic acid treatment and high-pressure washing with water for *C. intestinalis* (Carver et al. 2003; Carver et al. 2006; Ramsay 2008).

There is a need to compare the efficacy of treatments to find the best mitigation strategies in terms of time and frequency of treatment. A conventional approach involving field trials has been conducted for *C. intestinalis* (unpublished) and *B. violaceus* (Arens et al. 2011) to carry out such comparisons. However, these trials require considerable time to execute and are both cost and labour intensive. As an alternative, computer-based modelling can be used to mimic the population dynamics of a particular species (e.g. *C. intestinalis*) and subsequently to explore the likely effect of different control measures. While field-based experiments continue to provide a vital role, both in establishing the value of key parameters as specified within any model as well as in validating modelled outputs, a key advantage of such models is that they provide a mechanism to explore a range of possible intervention strategies in an inexpensive and timely manner.

Mathematical models are based on a set of equations with fixed parameters to describe a system. They have been applied to a wide range of problems associated with parasites and their control (Ebert et al. 2000; Jerwood and Saporu 1988; Luis et al. 2010; White et al. 2011). They can be used to represent complex phenomena and interactions, including those found in aquatic contexts (Fenton et al. 2006; Ford et al. 1999; Kanary et al. 2011; Murray 2011; Revie et al. 2005; Robbins et al. 2010; Thebault et al. 2007). These models typically predict the number of parasites/species of interest or the rates of change in the numbers of a species at a given time. Applying such approaches to model the population dynamics of *C. intestinalis* should provide the basis for a better understanding of population growth over time, as well as an ability to compare modelled results among various scenarios. The objective of this study was to develop a mathematical model that could describe the population dynamics of *C. intestinalis* in areas with mussel production, to better understand the growth of these populations under different temperature conditions.

Materials and methods

C. intestinalis *population dynamics*

The life cycle of *C. intestinalis* consists of egg, larva, recruit, juvenile, and adult stages. To capture the seasonal variation, six compartments representing the life stages of *C. intestinalis* were identified: egg (E), larva (L), recruit (R), juvenile (J), spring adult (A_{sp}), and autumn adult (A_{au}). Because surface area on which *C. intestinalis* can settle is a key determinant of population growth, two additional compartments to model dead stages were set up: dead juvenile (DJ) and dead adult (DA) (Figure 1). *Egg* refers to the *C. intestinalis* egg which has already been fertilized. *Larva* is the stage after the eggs hatch and become free-swimming larvae. *Recruit* refers to the tadpole that settles on a surface and develops through a process of metamorphosis. Those recruits that fail to metamorphose are assumed to detach from the surface. *Juvenile* is the stage at which the animal is completely metamorphosed but before it reaches sexual maturity. *Spring adult* refers to an animal that reaches its sexually mature size between May and September, and has the ability to reproduce. *Autumn adults* are animals that reach their adult stage between October and April. Two aggregate stages were also estimated: a surface-occupying stage (N_{SO}) and a visible surface-occupying stage (N_{VO}). N_{SO} comprises any individual that is attaching to the available surface, including R, J, A_{sp}, A_{au}, and the two dead stages, DJ and DA, which continue to occupy space regardless of their mortality status until they drop-off of the surface, releasing more space for recruits; while N_{VO}, which was only used for model validation purposes, represents

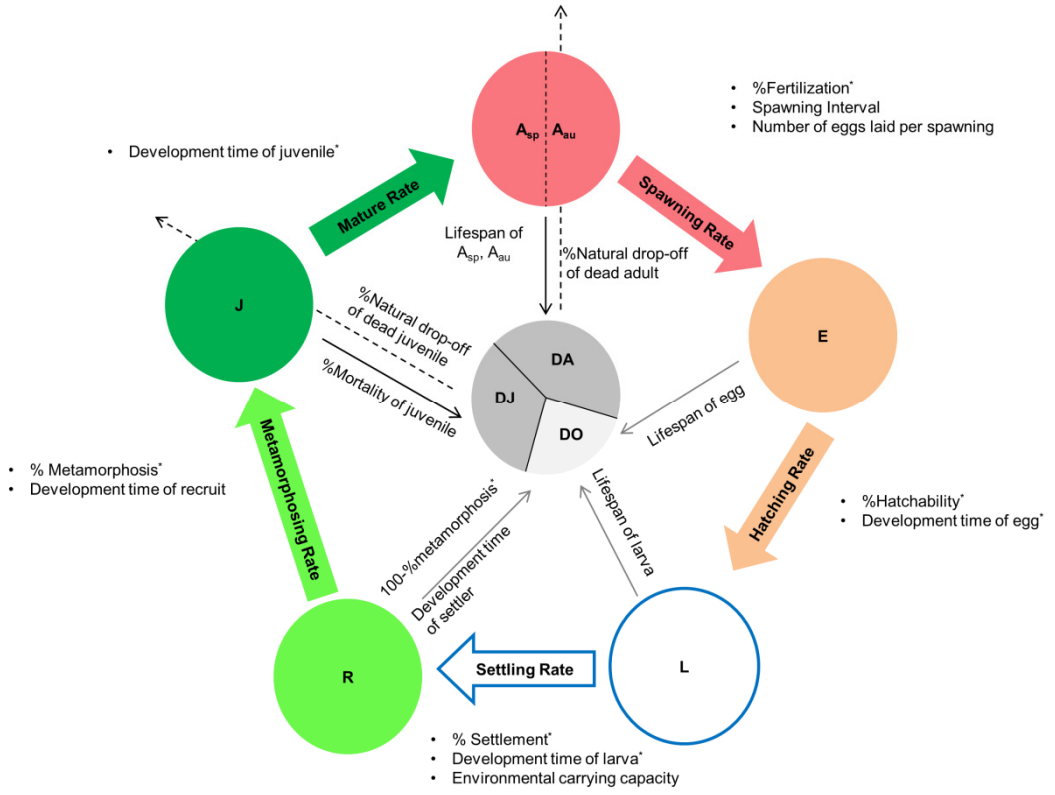

Figure 1. Diagram of *Ciona intestinalis* life cycle and parameters associating with flow rates. *A, E, L, R, J, DA, DJ*, and *DO* represent adult (spring and autumn), egg, larva, recruit, juvenile, dead adult, dead juvenile, and dead other stages. Asterisks (*) denote temperature-dependent parameters.

the total number of individuals in a visible stage; which are those included in N_{SO} but excluding recruits. The dead others stage (*DO*) in Figure 1 was not captured in the model since individuals transferred to this stage do not result in any reduction in settling surface.

A sexually mature adult *C. intestinalis* spawns eggs repeatedly throughout its lifespan (L_{Asp} days for spring adult and L_{Aau} days for autumn adult). On average, α eggs are released per individual every G_{SI} days. The eggs are then fertilized with sperm externally at the rate of $F_f(T^\circ)$. These fertilized eggs hatch at the rate of $F_h(T^\circ)$ and develop to larvae in $G_E(T^\circ)$ days. The egg is viable for up to L_E days before it is removed. After becoming a free-swimming larva, the tadpole turns into a recruit by finding a substrate to settle on at a percentage of $F_s(T^\circ)$ which is capacity dependent and is thus adjusted by a capacity adjusting factor ($\gamma(a,t)$; details in a subsequent section). The larval phase can last for up to $G_L(T^\circ)$ days before settling and larva that do not settle in L_L days will die. The recruit stage takes G_R days to metamorphose to become a juvenile. The percentage of recruits that undergo the metamorphosis process is $F_m(T^\circ)$, whereas 1-$F_m(T^\circ)$ of recruits die in G_R days. Each individual in the juvenile stage takes $G_J(T^\circ)$ days to become a sexually mature adult and has a daily mortality rate of m_J. Space occupancy is released through a drop-off process, which occurs at the daily rates of μ_{DJ} and μ_{DA} for dead juveniles and dead adults, while juveniles and adults drop-off of mussel sock at the daily rates of μ_J and μ_A. A dichotomous variable, x, was used to control whether adult can produce eggs with the cut-off temperature at 4˚C (*Eq. 1*; Table 1). A similar approach was applied for spring and autumn adult

Table 1. List of mathematical equations for *Ciona intestinalis* population dynamic model including differential equations, temperature model, capacity adjusting factor, and average relative sensitivity function.

Mathematical equations	Number
$\frac{dE(t)}{dt} = \frac{(x\times\alpha)\times F_f(T°)}{G_{SI}} \times \left(A_{sp}(t) + A_{au}(t)\right) - \frac{F_h(T°)}{G_E(T°)} \times E(t) - \frac{E(t)}{L_E}$; $x = \begin{cases} 0, & T° < 4°C \\ 1, & T° \geq 4°C \end{cases}$	*Eq. 1*
$\frac{dL(t)}{dt} = \frac{F_h(T°)}{G_E(T°)} \times E(t) - \frac{F_s(T°)}{G_L(T°)} \times \gamma(a,t) \times L(t) - \frac{L(t)}{L_L}$	*Eq. 2*
$\frac{dR(t)}{dt} = \frac{F_s(T°)}{G_L(T°)} \times \gamma(a,t) \times L(t) - \frac{F_m(T°)}{G_R} \times R(t) - \frac{1-F_m(T°)}{G_S} \times R(t)$	*Eq. 3*
$\frac{dJ(t)}{dt} = \frac{F_m(T°)}{G_R} \times R(t) - \frac{J(t)}{G_J(T°)} - m_J \times J(t) - \mu_J \times J(t)$	*Eq. 4*
$\frac{dA_{sp}(t)}{dt} = \frac{J(t)}{G_J(T°)} \times y - \frac{A_{sp}(t)}{L_{A_{sp}}} - \mu_A \times A_{sp}(t)$; $y = \begin{cases} 0, & t > 120 \\ 1, & t \leq 120 \end{cases}$	*Eq. 5*
$\frac{dA_{au}(t)}{dt} = \frac{J(t)}{G_J(T°)} \times (1-y) - \frac{A_{au}(t)}{L_{A_{au}}} - \mu_A \times A_{au}(t)$; $y = \begin{cases} 0, & t > 120 \\ 1, & t \leq 120 \end{cases}$	*Eq. 6*
$\frac{dDJ(t)}{dt} = m_J \times J(t) - \mu_{DJ} \times DJ(t)$	*Eq. 7*
$\frac{dDA(t)}{dt} = \frac{A_{sp}(t)}{L_{A_{sp}}} + \frac{A_{au}(t)}{L_{A_{au}}} - \mu_{DA} \times DA(t)$	*Eq. 8*
$T° = \beta_0 + \sum_{j=1}^{J} \beta_{s_j} \sin\left(\frac{2j\pi t}{p}\right) + \sum_{j=1}^{J} \beta_{c_j} \cos\left(\frac{2j\pi t}{p}\right)$	*Eq. 9*
$T° = A \times \sin\left(\frac{2\pi t}{p} + \alpha\right) + C$	*Eq. 10*
$\gamma(a,t) = 1 - \frac{N_{SO}(t)}{K \times a}$	*Eq. 11*
$\bar{S}_p^F = \frac{\overline{\%\ change\ in\ F(t)}}{\%\ change\ in\ p} = \frac{\sum_{t=0}^{T} \left[\frac{F(t) - F_b(t)}{F_b(t)}\right] / T}{\left\lvert\frac{\Delta p}{p}\right\rvert}$	*Eq. 12*

compartments (Eq. 5 and 6; Table 1). A dichotomous variable, *y*, was created to define whether the model was in spring (y=1) or autumn season (y=0). This allows the model to assign animals from juvenile stage to spring or autumn adult compartments depending on time of the model. The *C. intestinalis* life cycle can be described by a set of differential equations (*Eq. 1-8*; Table 1). The model was set to run for one calendar year, with Day 1 being the 1st of May until the termination of the model at Day 365 and was initialized with an initial autumn-adult presence of 0.002 individual·cm^{-2} (or approximately 12 adults per mussel sock) based on field observations made by the Atlantic Veterinary College (AVC) shellfish research group; all other life stages were initially set to zero. Spring was set to begin on the 1st of May and last for 120 days before switching to the autumn season. The model time step was set to 0.001 of a day.

Table 2. Parameter definitions, estimates, and parameter sources for *Ciona intestinalis* population dynamics model (Sources for temperature dependent parameters, which are marked with an asterisk, are shown in Tables S1 and S2.)

Parameter	Description	Value	Unit	Sources
$G_E(T^\circ)$	Development time of egg*	0.51 – 2.63	day	*
$G_L(T^\circ)$	Development time of larva*	0.31 – 10	day	*
G_R	Development time of recruit	12	day	Chiba et al. 2004
$G_J(T^\circ)$	Development time of juvenile*	30 – 90	day	*
G_{SI}	Spawning interval	3	day	Yamaguchi 1975; Carver et al. 2003
α	Number of eggs laid per spawning	1,000 – 1,500	egg	Carver et al. 2003
$F_f(T^\circ)$	%Fertilization*	0 – 85	%	*
$F_h(T^\circ)$	%Hatchability*	0 – 85	%	*
$F_s(T^\circ)$	%Settlement*	0 – 65	%	*
$F_m(T^\circ)$	%Metamorphosis*	0 – 80	%	*
L_E	Lifespan of egg	1.25	day	Svane and Havenhand 1993
L_L	Lifespan of larva	0.25 – 1.5	day	Havenhand and Svane 1991
L_{Asp}	Lifespan of Spring-Adult	150	day	Carver et al. 2006
L_{Aau}	Lifespan of Autumn-Adult	180	day	Yamaguchi 1975
m_J	% Mortality of juvenile	0.11	%	Svane 1984
μ_J	% daily drop-off of live juvenile	0	%	AVC shellfish research group pers. comm.
μ_A	% daily drop-off of live adult	0	%	AVC shellfish research group pers. comm.
μ_{DJ}	% daily drop-off of dead juvenile	0.05	%	AVC shellfish research group pers. comm.
μ_{DA}	% daily drop-off of dead adult	0.05	%	AVC shellfish research group pers. comm.
K	Environmental carrying capacity	40	individual·cm^{-2}	Ramsay et al. 2009

Parameter estimation

A total of 20 parameters were identified, with seven of these being temperature dependent (see Table 2 and Figure 1 for details). Parameters were estimated based on values reported in the scientific literature. In cases where a range was reported (e.g. number of eggs laid per spawning (α) and larval lifespan (L_L)) values were randomly selected from a uniform (for α) or triangular (for L_L) distribution, while for parameters derived from more than one source, the average value based on these sources was estimated. Similarly, the average values of estimates at different temperatures were determined for the temperature-dependent parameters, i.e. development times and percentage of individual successfully making the transition to a new phase for each stage (full details of the sources for these parameters are provided in Tables S1 and S2). All temperature-dependent parameters were linearly interpolated between reported values. Where no estimates could be found (e.g. temperatures less than 6 ˚C or greater than 24 ˚C in Figure 3) parameter values were assigned to the nearest reported value for %fertilization ($F_f(T^\circ)$), %hatchability ($F_h(T^\circ)$), %settlement ($F_s(T^\circ)$) and %metamorphosis ($F_m(T^\circ)$) (Figure 3), while values for development time of each stage were linearly extrapolated (Figure 2).

Temperatures

Average daily sea water temperatures were assumed to broadly follow trends that could be modelled by a sine wave and were estimated using trigonometric regression (Beer 2001; Cox 1987). The dependent variable was daily average temperature, whereas the independent variable was day of the year expressed in terms of sine and cosine functions, $\sin(2j\pi t/p)$ and $\cos(2j\pi t/p)$, where j is an integer, representing the number of sine and cosine terms, t represents day of the year ranging from 1 to 365, and p is the period, which is assumed to be 365 days in this model (*Eq. 9*; Table 1). The best fit temperature model was one comprising three sine/cosine terms (R-squared = 0.97). However for the sake of parsimony, a model with one sine and one cosine term was used (R-squared = 0.95). After acquiring the regression coefficients, the model was simplified to the simple sine function in *Eq. 10* (Table 1) to allow for a supple parameter. Amplitude (A) is computed as

$$\sqrt{\beta_{S_j}^2 + \beta_{C_j}^2}$$

while the shift parameter (α) is $\tan^{-1}(\frac{\beta_C}{\beta_S})$, and the constant ($C$) is equal to β_0.

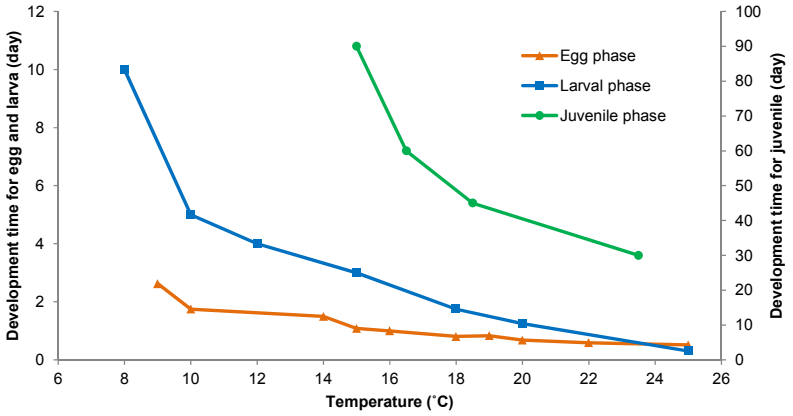

Figure 2. Reported values and linear interpolants of development time (day) at different temperatures for egg ($G_E(T^\circ)$), larval ($G_L(T^\circ)$), and juvenile ($G_J(T^\circ)$) phases.

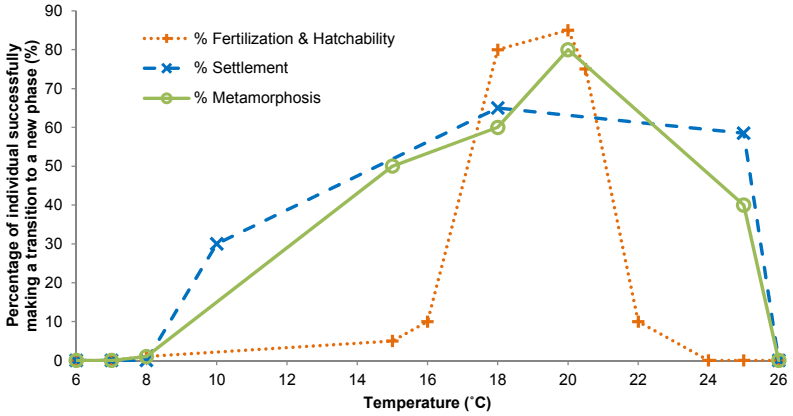

Figure 3. Reported values and linear interpolants for percentage of individual successfully making a transition to a new phase: %fertilization ($F_f(T^\circ)$), %hatchability ($F_h(T^\circ)$), %settlement ($F_s(T^\circ)$), and %metamorphosis ($F_m(T^\circ)$) at different temperatures.

Environmental carrying capacity

The model assumes that the settling rate of larvae is density dependent, varying with the proportion of $N_{SO}(t)$ to environmental carrying capacity (K) of a surface area a, which is the maximum number of *C. intestinalis* that the system can accommodate per cm^2 multiplied by the total surface area (a cm^2) of mussel socks in a bay. The model used an estimate of 40 individuals per cm^2 (Ramsay et al. 2009) for K. Mussel sock density in PEI was estimated to be 630 mussel socks per acre in the 500-acre bay of Georgetown Harbour (AVC shellfish research group pers. comm.). Each mussel sock was assumed to have a cylindrical shape with a length of 180 cm and a diameter of 10 cm. The capacity adjusting factor $\gamma(a,t)$ is the proportion of available surface area to the total surface area at time t. It is used to adjust the settling rate and is defined in *Eq. 11* (Table 1).

Model validation

Model fit was assessed by comparing the modelled number of each *C. intestinalis* life stage to observed field data collected by the AVC shellfish research group during May to November in 2008 at Georgetown Harbour, PEI. Two datasets relating to larval concentration, and population development were used in the assessment. A third dataset, population recruitment, is provided in the supplementary materials.

For larval concentration, data collection was carried out using the larval sampling method described in Ramsay (2008). In brief, a 150-litre water sample in the water column between water surface and the first 2 meter depth was collected using bilge pump every two weeks from the study area and concentrated to 10 millilitres. This was then evaluated under a stereo microscope to identify and estimate the number of larvae. The data thus provided a representation of larval

concentrations across the season. Due to these differences in measurement scale, direct comparison between the modelled output and observed data was not carried out and validation was based on a comparison of temporal patterns.

For population development, the number of *C. intestinalis* accumulating during the reproductive season was investigated by deploying fifteen 100 cm^2 PVC plates at 2–3 meter depth below the water surface on May 1st, 2008. One plate was then randomly retrieved every two weeks to evaluate the numbers of *C. intestinalis* present at that time point. The samples were visually evaluated, so individuals smaller than 5 mm were not included in the count (for details see Ramsay et al. 2009). The data thus represented the total number of settled *C. intestinalis* per cm^2 over the season which was compared to the modelled N_{VO}. Based on the extensive field experience of one of the co-authors (Davidson) it was estimated that only around half of the juvenile population would be visually detectable in a field setting and that the dead recruit stages do not take up space since they detach from the surface after they die.

Population recruitment data were collected according to the method used by Ramsay et al. (2009). PVC plates measuring 100 cm^2 were left at 2–3 meter depth below the water and retrieved after a two-week period. The numbers of recruiting *C. intestinalis* were identified under a dissecting microscope. This procedure was repeated every two weeks over the study period (May to November, 2008). These data provide estimates of the numbers of early recruiting *C. intestinalis* over time, but can only sensibly be compared to the modelled numbers in the recruit stage for the initial two weeks when the recruitment occurred.

Sensitivity analysis

Sensitivity analysis was carried out to analyse the influence of each parameter on the N_{SO} using a relative sensitivity function (S_p^F) which is the percentage of change in modelled output relative to a certain percent change in input. Each parameter (p) was increased or decreased by 20% of its default value one at a time, except for L_{Asp} and L_{Aau} that were changed simultaneously. S_p^F was calculated and averaged over time to obtain an average relative sensitivity index ($\bar{S}_p^F$) for each parameter (*Eq.12*; Table 1). *F(t)* denotes modelled N_{SO} at any time t when a parameter value is varied, while $F_b(t)$ refers to the modelled N_{SO} when all parameters were set to their default values.

What-if scenarios

Four temperature conditions were modelled for what-if scenarios: baseline (replicating the temperature from Georgetown Harbour in 2008), cold year, long summer, and warm summer. Three parameters with high $\bar{S}_p^F$ values, together with environmental carrying capacity and the drop-off rates of live juvenile and adult stages were further evaluated for their influences on N_{SO}. These parameters were varied by a 20% increase or decrease on their default values and the outcomes assessed under the four temperature conditions.

Results

The observed and modelled average daily temperatures of Georgetown Harbour from May 2008 to May 2009 are illustrated in Figure 4. The modelled temperature was 3.3 ˚C at the start of the model with a mean of 7.1 ˚C, had a minimum of -2.7 ˚C and reached a maximum of 16.9 ˚C in late August.

The modelled total number of egg (eggs$\times 10^9$), larva (larvae$\times 10^9$), as well as the abundances per cm^2 of recruit, juvenile, adult, and visible occupying stages (N_{VO}) are illustrated in Figures 5–9. Each stage started to become active in early June when the temperature reached 8 ˚C, but the numbers were so low that they can hardly be detected in the summary plots. The modelled numbers of eggs rose from mid-August and reached a peak of 47×10^9 eggs in mid-October (Figure 5). The number of larvae began to increase just after the rise in egg abundance, as would be expected, reaching a peak of 4.8×10^9 larvae around mid-September at around the same time as the observed larval counts reached their maximum (Figure 6). The shapes of the observed and modelled larvae abundance over time are broadly similar though there is a limitation in comparing their magnitudes, as the two quantities are represented on quite different scales. Recruits followed a similar pattern to larvae, once again reaching a peak (4.5 recruit·cm^{-2}) in mid-September (Figure 7). The abundance of juveniles began to rise in late August and reached its peak (4.3 juvenile·cm^{-2}) in early October, while the abundance of adults increased from early September and reached the highest levels (1.9 adult·cm^{-2}) in mid-December (Figure 8). A comparison between N_{VO} for the

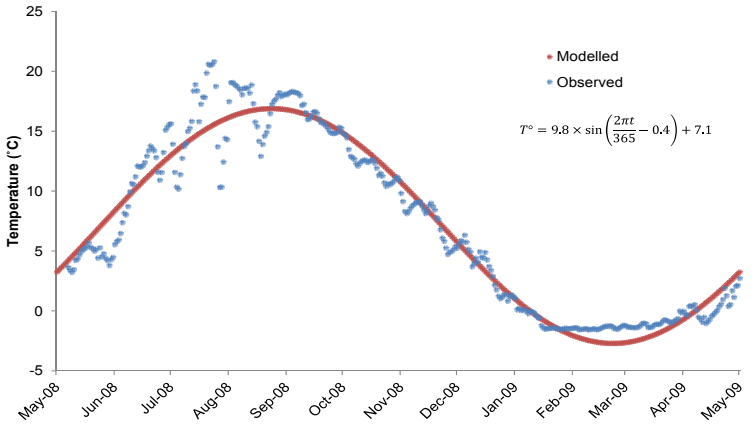

Figure 4. The observed and modelled average daily temperatures of Georgetown Harbour from May 2008 to May 2009.

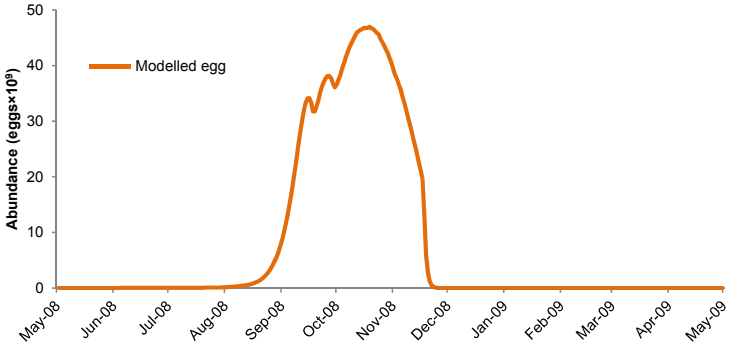

Figure 5. The modelled abundance of *Ciona intestinalis* at egg stage in Georgetown Harbour from May 2008 to May 2009.

observed and modelled data is shown in Figure 9. The observed N_{VO} gradually increased from late July until mid-October with a rapid increase in late October. The modelled N_{VO} broadly followed the shape of the observed curve, reaching a plateau at an abundance of around 5 individ.·cm^{-2}. However, the modelled N_{VO} started to increase a month later than the observed data and showed a much more rapid rise after this initial increase than was the case for the observed data.

The modelled outputs using parameters fitted to the observed temperatures are presented in Figures S1–S5. The outputs of each stage appear to show an initial peak or early rise around late July (recruit and juvenile stages) to early August (egg, larval, adult, and N_{VO} stages). Additionally, the modelled outputs (bases observed temperature) result in values around 5–6 times higher than those seen in the outputs using a simple sine curve-based temperature model and as high as two orders of magnitude for egg and larval stages.

Figure 10 demonstrates the average relative sensitivity indices ($\bar{S}_p^F$) calculated from *Eq. 12* (Table 1) for the 20% increase/decrease models at the baseline temperature. It shows the impact of changes in parameter values on the modelled output. The further the value of $\bar{S}_p^F$ is from zero, the more influential a parameter is. The sign of $\bar{S}_p^F$ explains the direction of the modelled output with respect to changes in an input parameter. For instance, the $\bar{S}_p^F$ of 2.88 associated with a 20% decrease in spawning interval, the most influential parameter to the model (Figure 10), will generate on average a modelled output (N_{SO}) that is 57.6% higher than when the default parameters are used. In contrast, the effect of increasing the spawning interval by 20%, will generate a 28.8% decrease in the output. It can also be seen that the sensitivity in modelled output to changes of up to 20% in the mortality rate of juveniles and natural drop-off of dead

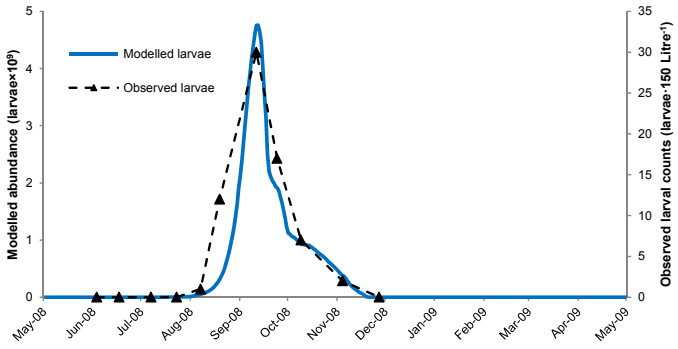

Figure 6. The modelled abundance of *Ciona intestinalis* at larval stage compared to observed larval counts (per 150 Litre) from Georgetown Harbour during May to November 2008.

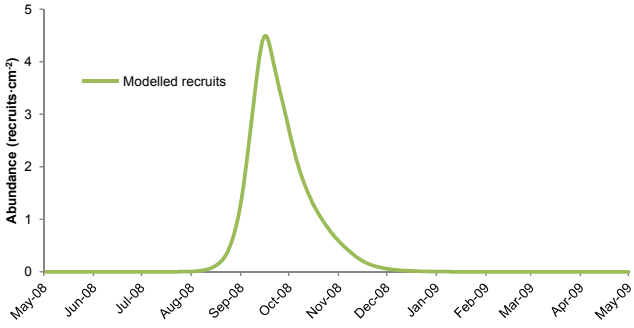

Figure 7. The modelled abundance of *Ciona intestinalis* at recruit stage from Georgetown Harbour during May 2008 to May 2009.

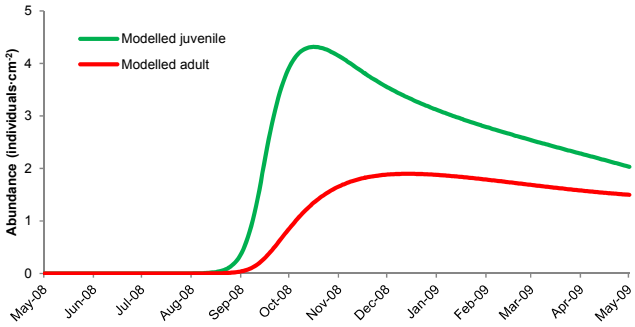

Figure 8. The modelled abundance of *Ciona intestinalis* at juvenile and adult stages in Georgetown Harbour from May 2008 to May 2009.

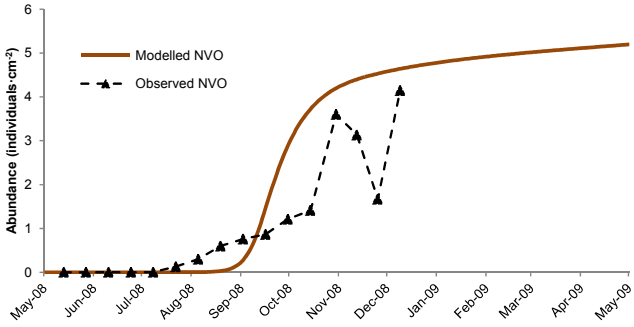

Figure 9. The modelled abundance of *Ciona intestinalis* at the aggregate visible occupying stage (N_{VO}) (half of juveniles, adults, and dead juveniles and adults) compared to the observed population developmental data collected from Georgetown Harbour during May to December 2008.

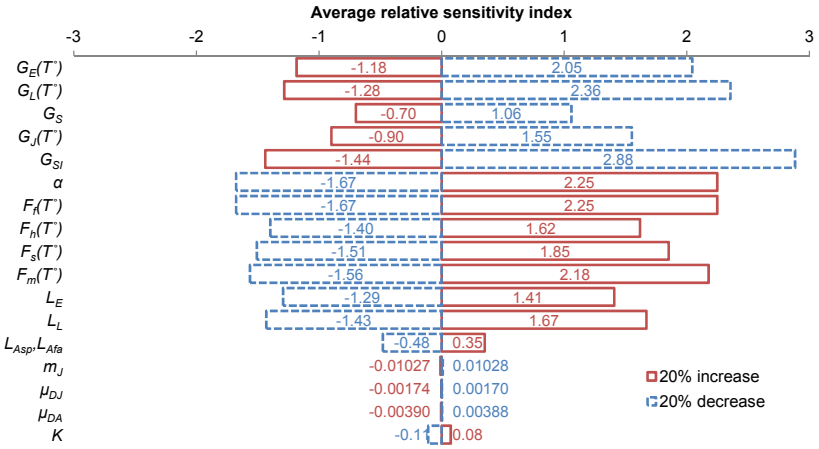

Figure 10. Average relative sensitivity index (S_p^F) for 20% increase/decrease models (Acronyms are detailed in Table 2).

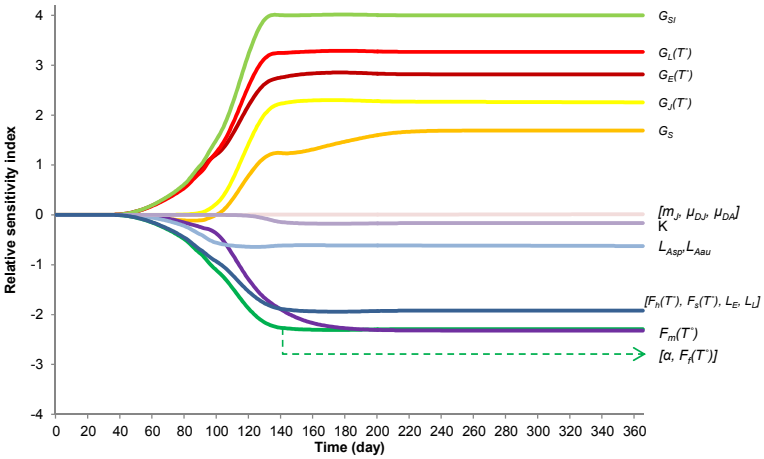

Figure 11. Relative sensitivity index [S_p^F] over time for variation (20% decrease) of different parameters of the *Ciona intestinalis* population dynamics model for Georgetown harbour during May 2008 to May 2009 (Acronyms are detailed in Table 1).

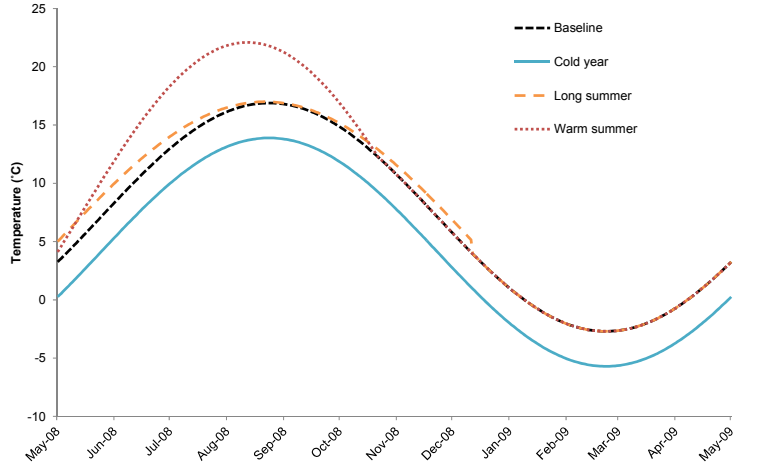

Figure 12. The modelled temperatures for 4 different conditions: baseline (replicating temperature from Georgetown Harbour in 2008), cold year, long summer, warm summer.

juveniles and adults was very low, with $\bar{S}_p^F$ values close to zero (Figure 10). The effects of any two parameters can be compared by dividing $\bar{S}_p^F$ of one parameter by the other. For example, the effect of a 20% reduction in $G_L(T^\circ)$ is 1.15 times greater than the effect of a 20% reduction in $G_E(T^\circ)$. To show the temporal variation of relative sensitivity index (S_p^F), which cannot be seen in Figure 10, the plot of S_p^F for each parameter over time when parameters were decreased by 20% is also shown (Figure 11). It is not until Day 40 that the S_p^F values start to show an increase or decrease, and this change continued up to around Day 160, after which point they remained constant. Parameters with positive S_p^F such as those related to the development time appeared to have higher magnitudes when compared to those with negative values (Figure 11). Mapping S_p^F values over time for a 20% decrease in parameter values, indicates a similar and opposite trend to those found for the 20% increase model (data not shown).

The four temperature scenarios explored are shown in Figure 12. Figure 13 illustrates the N_{SO} stages for a baseline temperature scenario based on 20% variation in three parameters with high $\bar{S}_p^F$ values: spawning interval (G_{SI}), development time of larva ($G_L(T^\circ)$), and number of laid eggs per spawning (α), as well as an increase to 1% and 2% of the drop-off of live juvenile and adult (μ_J, μ_A). As expected, increases in G_{SI} or $G_L(T^\circ)$ caused a reduction in N_{SO}, while an increase in α increased the N_{SO} compared to default value (see Figure 13). However, when these variations were explored in a warm summer year (data not shown) the overall change in N_{SO} was marginal by comparison. Similarly changes in environmental carrying capacity (K) resulted in little or no change in N_{SO} stages for baseline and cold year scenarios. On the other hand there were more pronounced changes in the output for both long and particularly warm summer scenarios (Figure 14) when K was altered. The results also indicate that the model is highly sensitive to changes in temperature condition. Looking at the default values (dash lines in Figure 14), the modelled N_{SO} varied from only 0.004 individuals·cm^{-2} in a cold year (Figure 14B) to the maximum capacity of 40 individuals·cm^{-2} in a warm summer (Figure 14D). Figure 15 applied variation to the %drop-off of live juvenile and adult (μ_J and μ_A) to demonstrate its effect under different temperature conditions on the N_{SO} stages. When comparing %drop-off between the two temperature conditions, warm summer showed higher N_{SO} than long summer for every level of %drop-off. Additionally, the decrease in N_{SO} for a warm summer occurred later and with a larger relative change than was observed for the long summer scenario.

Discussion

The *C. intestinalis* populations model has demonstrated a capacity to address a number of the objectives of this study. It is flexible and can be adapted to a range of different temperature conditions. The model, in general, provided similar outputs to the observed data based on a comparison of temporal patterns. Although differences in scale between the observed and modelled larval counts prevented any direct comparison, the model provided an accurate prediction as to the timing of both the growth and the decline of the larval stage.

For the recruit stage focussing on the first two weeks of recruitment period, the model using a simple sine curve to represent sea water temperature was unable to capture an initial moderate rise in mid-July. The likely explanation for this is that the temperature model did not capture the high temperatures seen during late June and July which would have affected the settling rate. When fitted to the observed temperature profile from Georgetown Harbour in 2008, as opposed to the simulated baseline (sine-wave model), the model was able to capture this initial rise in the recruit population (Figure S3).

A separate study of recruitment patterns of *C. intestinalis* took place in the Montague River, PEI in 2006 (Ramsay et al. 2009). The observed water temperature from the end of May to December in 2006 ranged from 6 ˚C to 18 ˚C which was quite similar to the modelled baseline temperature used in our study, though the model estimates were consistently around 1 ˚C lower. This field study reported the first recruitment of recruits in the second week of June when the temperature was nearly 9 ˚C and found one recruitment peak when the temperature was at its maximum (17.7 ˚C) in late August. Our model indicated a similar single recruitment peak pattern, though the peak was reached around one month later as the temperatures were not so high in the current study as compared to temperatures in the Montague River in 2006. This supports the argument that the model can adequately predict the recruitment timing of *C. intestinalis* given suitable temperature profiles.

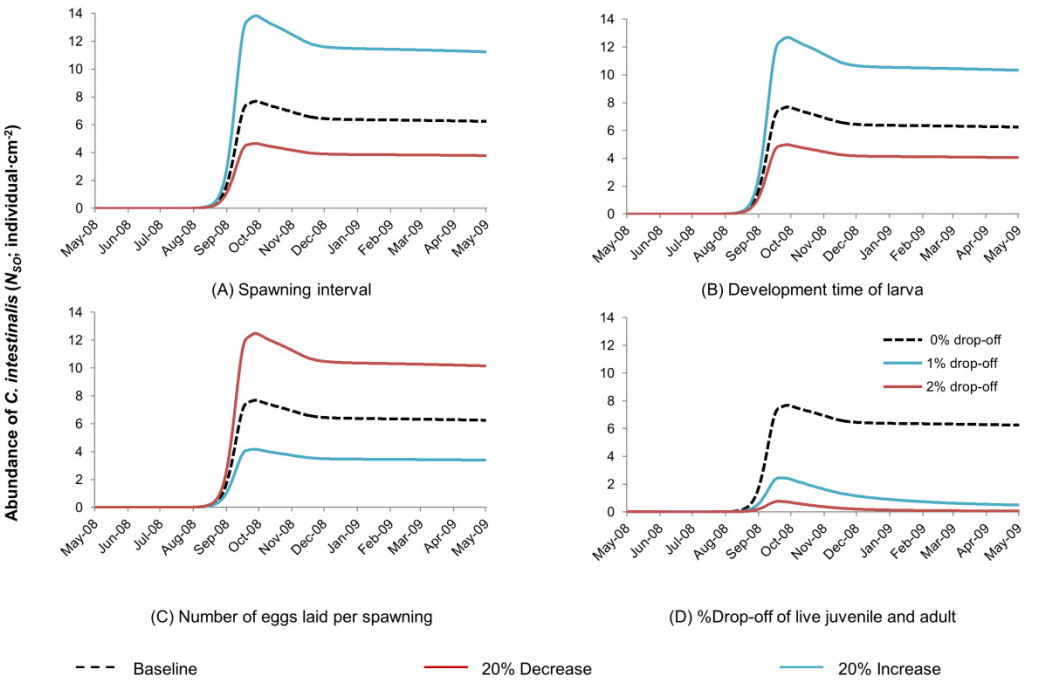

Figure 13. Impact on main outcome (N_{SO}) of parameter variation in (A) spawning interval (G_{SI}), (B) development time of larva ($G_L(T^\circ)$), (C) number of eggs laid per spawning (α), and (D) %drop-off of live juvenile and adult (μ_I and μ_A) at baseline temperature.

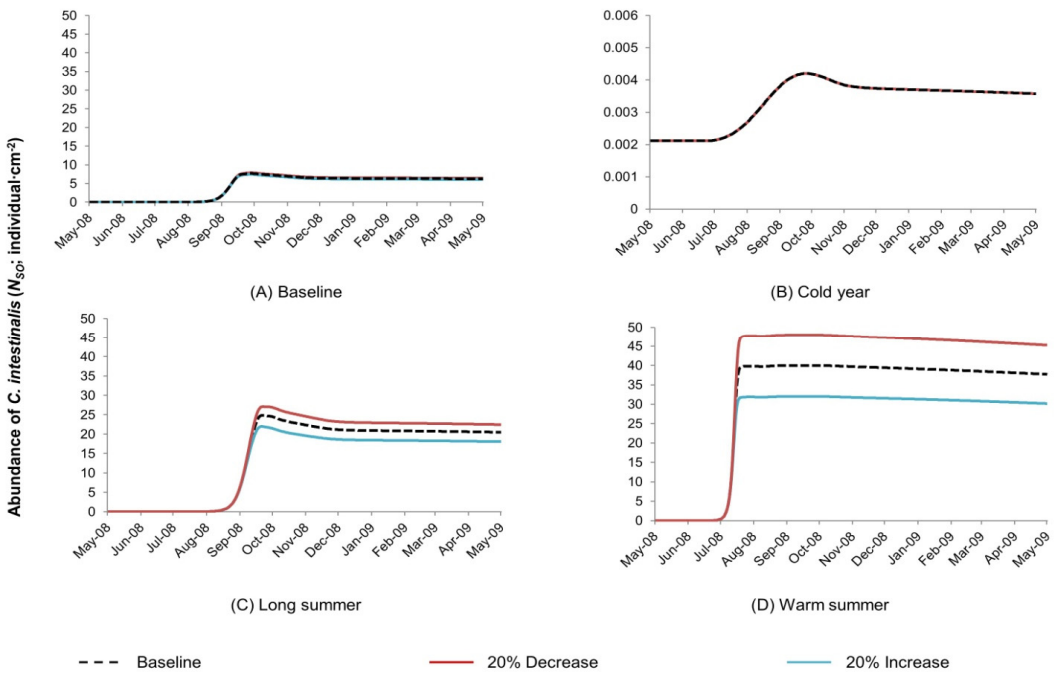

Figure 14. Impact on main outcome (N_{SO}) of variation in environmental carrying capacity (K) at different temperature scenarios: (A) baseline, (B) cold year, (C) long summer, and (D) warm summer.

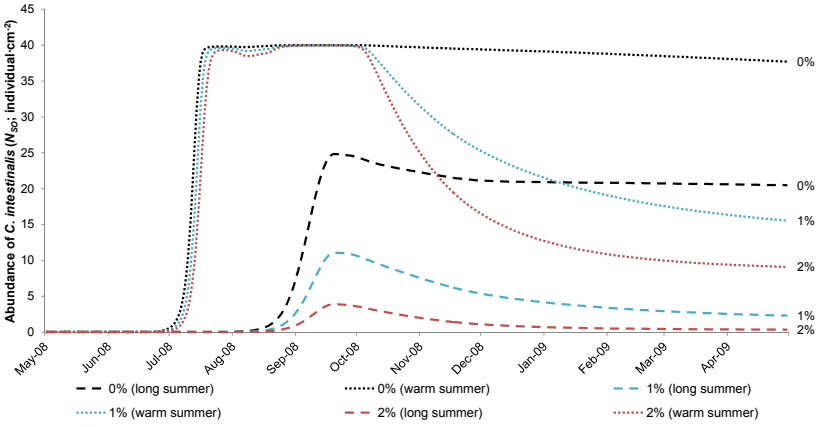

Figure 15. Impact on main outcome (N_{SO}) of variation in percentage drop-off of live juvenile and adult (μ_J and μ_A) (0%, 1% and 2%) in long summer and warm summer scenarios.

As noted in Materials and Methods, comparing the observed and modelled recruitment data cannot strictly be justified, except during the first two weeks when recruitment occurs. This is due to the fact that in the observed data the surface on which recruits were counted was always based on fresh plate, which would result in higher estimations of settling rate when compared to the modelled data. Furthermore the study design used to collect the observed recruitment data performed sampling every two weeks, which may not be frequent enough as the larval stage will last for only around 10 days at the temperatures involved. In addition our model assumes that there was no external pressure affecting the modelled population, i.e. that all recruits derive from eggs and larvae produced by modelled adults in the population. However, within the observed data such external pressures are unknown and may therefore result in significant differences between the observed and modelled data.

The population development data (detailed in materials and methods) represented *C. intestinalis* stages that were attached on a surface and were of detectable size (larger than 5 mm) over the season. Due to the limitation of information on the life stages in the observed data (i.e. proportions of each stage were not identified) it was not easy to compare the modelled visible surface occupying stages to this dataset by simply adding up the numbers of juvenile, adult, dead juvenile and adult stages, since the modelled juveniles might have included individuals that were less than 5 mm in size. To validate the model against this population development data, the model was built under the assumption that only half of the juvenile stage individuals would be of detectable size. The model did not reflect the modest rise in N_{VO} seen early in the season in the observed data for the same reason that it could not simulate the initial rise of recruits, which are the source of juveniles, as discussed previously. The model also illustrated that the population remained relatively static after its peak in the middle of October. The abundance stopped increasing because the individual growth rate of *C. intestinalis* in cold temperatures is very low (Dybern 1965; Yamaguchi 1975), yet it did not significantly decrease because the drop-off of dead individuals is also low (AVC shellfish research group pers. comm.).

Temperature was modelled using a single sine term, though an equation utilising three sine terms provided a better fit. This was because the study aimed to create a model that explains how *C. intestinalis* populations behave under a range of temperature conditions, which requires a model that can be easily modified to different contexts and is not over-fitted to one specific set of temperatures. On the other hand, if the objective is to make specific predictions, real water temperature data from a given year or season may provide better results. The single sine term model provides the flexibility of changing parameter values in a sensible way, but in this case study failed to capture the higher temperatures that occurred during July and early August which will influence the modelled temperature-dependent flow rates. However, fitting the parameters to the observed temperatures resulted in an earlier increase in the population of each stage (when compared to those seen using the simple temperature

model); indicating that the model can produce adequate outputs for different temperature scenarios.

The estimation of temperature-dependent parameters assumed linear interpolations when no values were reported between 6 ˚C and 26 ˚C. Where temperature was beyond this range, imputation, using either the nearest value or linear extrapolation, was carried out. As can be seen from Figure 2, a reasonable number of estimates exist at a range of temperatures for development times of egg, larval and juvenile stages which allowed for a sensible degree of interpolation, except at lower temperatures. However, there appeared to be more discontinuity when considering estimates of the percentage of individual successfully making the transition to a new phase for various life stages (Figure 3) and therefore the interpolations adopted are inevitably more open to debate and refinement. In practice this was only a concern at lower temperature as sea water temperatures in the PEI coastal area rarely rise above 23 ˚C. Nonetheless, a reasonable amount of evidence that *C. intestinalis* do not develop at temperatures below 6 ˚C mitigates this as a serious concern.

The plateau patterns observed in the modelled output (Figure 9 and 13–15) were a consequence of two factors: temperature and space availability. At high temperatures, the life stages grow quickly and rapidly reach maximum capacity. Although the population can still grow, there is no space available to accommodate the new recruit stages. In low to moderate temperatures (e.g. the modelled baseline and cold year scenarios), the population tends to grow more slowly. In these scenarios the maximum capacity is not reached prior to a time at which the temperature begins to decrease and thus limits the growth in the population. This strong relationship between growth rate and temperature is a characteristic of ectothermic organisms (Guarini et al. 2011), such as *C. intestinalis*. Under warm weather conditions such as the warm summer scenario presented in this study, the populations will grow faster and reach the maximum capacity very quickly (Gillooly et al. 2001). In contrast, when modelling the population under a cold weather scenario very few individuals successfully develop, indicating that the temperatures observed in this study represent values close to the lower thermal range limit for *C. intestinalis*. This is in agreement with Dybern (1965) who found no Ciona species in the sub-Arctic and Arctic regions, where temperature records are seldom higher than 3–4 ˚C

This study used a relative sensitivity function to evaluate the influence of changes in parameter values on the overall outcomes of the model. Although this method is known to have limitation, it is a relatively simple way to compare the effects of different parameters (Smith et al. 2008). Under the baseline temperature scenario, the model is particularly sensitive to development time and percentage of individual successfully making the transition to a new phase early life stages (i.e. egg and larva), as well as to spawning interval and number of eggs laid per spawning. As expected increasing spawning interval or development time slows down the growth of the *C. intestinalis* population, while increasing the number of eggs laid per spawning positively affects population growth. The sensitivity of the model to changes in the percentage drop-off of dead juvenile and dead adult stages was low; however, these drop-off rates only relate to the dead stages. A range of mitigation strategies to control *C. intestinalis* focusing on the removal of the occupying stages have been suggested elsewhere (Carver et al. 2003; Carver et al. 2006; Edwards and Leung 2009; Gill et al. 2007). The predictions from this model suggest that changes in environmental carrying capacity have a larger impact on population growth under warm summer or long summer-like conditions as compared to what would be the case in cold years. Although drop-off of live *C. intestinalis* rarely occurs naturally (AVC shellfish research group pers. comm.), the model indicates that changes in this parameter can have major impacts on modelled outputs. The results suggest that increased drop-off of live *C. intestinalis,* as would be the case under certain mechanical treatments, can act to limit population growth and is worthy of further investigation in combination with space and time control.

The use of this model is currently limited to a one-year scenario. To use this model for multi-year scenarios, factors related to mortality during the winter would be required to adequately model the correct number of initial adults at the start of a new yearly cycle. The population may increase exponentially in a subsequent year if there is very low mortality during winter. On the other hand if high mortality of adults occurs there would be few initial adults to initiate the reproduction cycle, resulting in an outcome not dissimilar to the single year scenario modelling in this paper. Therefore, the effects of temperature on physiological rates and development stages of

this species, particularly in the colder winter months, require further study.

Overall, this mathematical model provides reasonable predictions around the dynamics of *C. intestinalis* populations on mussel farms in PEI. This approach should prove useful for farm management and can be adapted to model populations in different region or of other invasive species. Future studies will explore its application to an evaluation of the effectiveness of combining treatment and space management at different temperature profiles to develop mitigation strategies for the control of *C. intestinalis* populations and to improve bay management plans that might be implemented by mussel producers.

Acknowledgements

The authors thank the AVC shellfish research group and the AVC modelling group for technical assistance. The study was supported as part of a research project funded by the Atlantic Innovation Fund (Atlantic Canada Opportunity Agency) and the 2010 AVC Research Fund. Thanks are also due to the three anonymous reviewers who provided thoughtful comments on earlier versions of the manuscript.

References

Arens CJ, Paetzold SC, Ramsay A, Davidson J (2011) Optimization of pressurized seawater as an antifouling treatment against the colonial tunicates *Botrylloides violaceus* and *Botryllus schlosseri* in mussel aquaculture. *Aquatic Invasions* 6: 465–476, http://dx.doi.org/10.3391/ai.2011.6.4.12

Baghdiguian S, Martinand-Mari C, Mangeat P (2007) Using Ciona to study developmental programmed cell death. *Seminars in Cancer Biology* 17: 147–153, http://dx.doi.org/10.1016/j.semcancer.2006.11.005

Beer WN (2001) Six parameter water temperature model. Columbia Basin Research. http://www.cbr.washington.edu/sites/default/files/documents/six.param.white.pdf (Accessed 3 March 2013)

Bellas J, Vázquez E, Beiras R (2001) Toxicity of Hg, Cu, Cd, and Cr on early developmental stages of *Ciona intestinalis* (Chordata, Ascidiacea) with potential application in marine water quality assessment. *Water Research* 35: 2905–2912, http://dx.doi.org/10.1016/S0043-1354(01)00004-5

Bellas J, Beiras R, Vázquez E (2003) A standardisation of *Ciona intestinalis* (Chordata, Ascidiacea) embryo-larval bioassay for ecotoxicological studies. *Water Research* 37: 4613–4622, http://dx.doi.org/10.1016/S0043-1354(03)00396-8

Berrill NJ (1947) The development and growth of Ciona. *Journal of the Marine Biological Association of the United Kingdom* 26: 616–625, http://dx.doi.org/10.1017/S0025315400013825

Carver CE, Chisholm A, Mallet AL (2003) Strategies to mitigate the impact of *Ciona intestinalis* (L.) biofouling on shellfish production. *Journal of Shellfish Research* 22: 621–631

Carver CE, Mallet AL, Vercaemer B (2006) Biological synopsis of the solitary tunicate *Ciona intestinalis*. Canadian Manuscript Report of Fisheries and Aquatic Sciences, Dartmouth, Nova Scotia, 55 pp

Chiba S, Sasaki A, Nakayama A, Takamura K, Satoh N (2004) Development of *Ciona intestinalis* juveniles (through 2nd ascidian stage). *Zoological Science* 21: 285–298, http://dx.doi.org/10.2108/zsj.21.285

Cirino P, Toscano A, Caramiello D, Macina A, Miraglia V, Monte A (2002) Laboratory culture of the ascidian *Ciona intestinalis* (L.): a model system for molecular developmental biology research. Marine Models Electronic Record. http://hermes.mbl.edu/BiologicalBulletin/MMER/cirino/CirTit.html#I (Accessed 30 January 2013)

Cox NJ (1987) Speaking Stata: In praise of trigonometric predictors. *Stata Journal* 6: 561–579

Dybern BI (1965) The life cycle of *Ciona intestinalis* (L.) f. typica in relation to the environmental temperature. *Oikos* 16: 109–131, http://dx.doi.org/10.2307/3564870

Ebert D, Lipsitch M, Mangin KL (2000) The effect of parasites on host population density and extinction: experimental epidemiology with *Daphnia* and six microparasites. *The American Naturalist* 156: 459–477, http://dx.doi.org/10.1086/303404

Edwards PK, Leung B (2009) Re-evaluating eradication of nuisance species: invasion of the tunicate, *Ciona intestinalis*. *Frontiers in Ecology and the Environment* 7: 326–332, http://dx.doi.org/10.1890/070218

Fenton A, Hakalahti T, Bandilla M, Valtonen ET (2006) The impact of variable hatching rates on parasite control: a model of an aquatic ectoparasite in a Finnish fish farm. *Journal of Applied Ecology* 43: 660–668, http://dx.doi.org/10.1111/j.1365-2664.2006.01176.x

Fisheries and Oceans Canada (2006) An economic analysis of the mussel industry in Prince Edward Island. Policy and Economics Branch, Gulf Region, Department of Fisheries and Oceans, Moncton, New Brunswick, 25 pp

Ford S, Powell E, Klinck J, Hofmann E (1999) Modeling the MSX parasite in eastern oyster (*Crassostrea virginica*) populations. I. Model development, implementation, and verification. *Journal of Shellfish Research* 18: 475–500

Gill K, MacNair N, Morrison A (2007) Investigation into the life cycle, impact on mussel culture and mitigation strategies for the vase tunicate (*Ciona intestinalis*), a new invasive species in the Montague/Brudenell River systems. PEI Department of Fisheries and Aquaculture Project 062AR20

Gillooly JF, Brown JH, West GB, Savage VM, Charnov EL (2001) Effects of size and temperature on metabolic rate. *Science* 293: 2248–2251, http://dx.doi.org/10.1126/science.1061967

Guarini JM, Chauvaud L, Cloern JE, Clavier J, Coston-Guarini J, Patry Y (2011) Seasonal variations in ectotherm growth rates: Quantifying growth as an intermittent non steady state compensatory process. *Journal of Sea Research* 65: 355–361, ttp://dx.doi.org/10.1016/j.seares.2011.02.001

Havenhand JN, Svane I (1991) Roles of hydrodynamics and larval behaviour in determining spatial aggregation in the tunicate *Ciona intestinalis*. *Marine Ecology Progress Series* 68: 271–276, http://dx.doi.org/10.3354/meps068271

Hendrickson C, Christiaen L, Deschet K, Jiang D, Joly JS, Legendre L, Nakatani Y, Tresser J, Smith WC (2004) Culture of adult ascidians and ascidian genetics. *Methods in Cell Biology* 74: 143–170, http://dx.doi.org/10.1016/S0091-679X(04)74007-8

Holmström C, Rittschof D, Kjelleberg S (1992) Inhibition of settlement by larvae of *Balanus amphitrite* and *Ciona intestinalis* by a surface-colonizing marine bacterium. *Applied and Environmental Microbiology* 58: 2111–2115

Hotta K, Mitsuhara K, Takahashi H, Inaba K, Oka K, Gojobori T, Ikeo K (2007) A web-based interactive developmental table for the ascidian *Ciona intestinalis*, including 3D real-image embryo reconstructions: I. From fertilized egg to hatching larva. *Developmental Dynamics* 236: 1790–1805, http://dx.doi.org/10.1002/dvdy.21188

Jackson A (2008) *Ciona intestinalis*. A sea squirt. Marine Life Information Network: Biology and Sensitivity Key Information Sub-programme [on-line]. Plymouth: Marine Biological Association of the United Kingdom. http://www.marlin.ac.uk/reproduction.php?speciesID=2991 (Accessed 8 December 2012)

Jerwood D, Saporu FWO (1988) Modelling endemic onchocerciasis in man in the presence of vector controls. *Medical Informatics* 13: 1–14, http://dx.doi.org/10.3109/14639238809003570

Kanary L, Locke A, Watmough J, Chasse J, Bourque D, Nadeau A (2011) Predicting larval dispersal of the vase tunicate *Ciona intestinalis* in a Prince Edward Island estuary using a matrix population model. *Aquatic Invasions* 6: 491–506, http://dx.doi.org/10.3391/ai.2011.6.4.14

Liu LP, Xiang JH, Dong B, Natarajan P, Yu KJ, Cai NE (2006) *Ciona intestinalis* as an emerging model organism: Its regeneration under controlled conditions and methodology for egg dechorionation. *Journal of Zhejiang University Science B* 7: 467–474, http://dx.doi.org/10.1631/jzus.2006.B0467

Locke A, Doe KG, Fairchild WL, Jackman PM, Reese EJ (2009) Preliminary evaluation of effects of invasive tunicate management with acetic acid and calcium hydroxide on non-target marine organisms in Prince Edward Island, Canada. *Aquatic Invasions* 4: 221–236, http://dx.doi.org/10.3391/ai.2009.4.1.23

Luis AD, Douglass RJ, Mills JN, Bjørnstad ON (2010) The effect of seasonality, density and climate on the population dynamics of Montana deer mice, important reservoir hosts for Sin Nombre hantavirus. *Journal of Animal Ecology* 79: 462–470, http://dx.doi.org/10.1111/j.1365-2656.2009.01646.x

MacNair N (2005) Invasive tunicates of concern for Prince Edward Island aquaculture. Charlottetown, Aqua Info Aquaculture Note. PEI Deparment of Agriculture, Fisheries and Aquaculture

Marshall DJ, Bolton TF (2007) Effects of egg size on the development time of non-feeding larvae. *The Biological Bulletin* 212: 6–11, http://dx.doi.org/10.2307/25066575

Murray AG (2011) A simple model to assess selection for treatment-resistant sea lice. *Ecological Modelling* 222: 1854–1862, http://dx.doi.org/10.1016/j.ecolmodel.2011.03.016

Ramsay A, Davidson J, Landry T, Arsenault G (2008) Process of invasiveness among exotic tunicates in Prince Edward Island, Canada. *Biological Invasions* 10: 1311–1316, http://dx.doi.org/10.1007/s10530-007-9205-y

Ramsay A, Davidson J, Bourque D, Stryhn H (2009) Recruitment patterns and population development of the invasive ascidian *Ciona intestinalis* in Prince Edward Island, Canada. *Aquatic Invasions* 4: 169–176, http://dx.doi.org/10.3391/ai.2009.4.1.17

Ramsay AP (2008) Vase tunicate, *Ciona intestinalis*: ecology and mitigation strategies. MSc Thesis, Atlantic Veterinary College, Department of Health Management. University of Prince Edward Island, Prince Edward Island, Canada, 120 pp

Revie CW, Robbins C, Gettinby G, Kelly L, Treasurer JW (2005) A mathematical model of the growth of sea lice, *Lepeophtheirus salmonis*, populations on farmed Atlantic salmon, *Salmo salar* L., in Scotland and its use in the assessment of treatment strategies. *Journal of Fish Diseases* 28: 603–613, http://dx.doi.org/10.1111/j.1365-2761.2005.00665.x

Robbins C, Gettinby G, Lees, F, Baillie M, Wallace C, Revie CW (2010) Assessing topical treatment interventions on Scottish salmon farms using a sea lice (*Lepeophtheirus salmonis*) population model. *Aquaculture* 306: 191–197, http://dx.doi.org/10.1016/j.aquaculture.2010.05.006

Smith ED, Szidarovszky F, Karnavas WJ, Bahill A (2008) Sensitivity analysis, a powerful system validation technique. *The Open Cybernetics and Systemics Journal* 2: 39–56, http://dx.doi.org/10.2174/1874110X00802010039

Statistics Canada (2012) Aquaculture statistics 2011. (catalogue number 23-222-X). Statistics Canada, Ottawa, Ontario

Svane IB (1984) Observations on the long-term population dynamics of the Perennial ascidian, *Ascidia mentula* O. F. Muller, on the Swedish west coast. *Biological Bulletin* 167: 630–646, http://dx.doi.org/10.2307/1541415

Svane IB, Havenhand JN (1993) Spawning and dispersal in *Ciona intestinalis* (L.). *Marine Ecology* 14: 53–66, http://dx.doi.org/10.1111/j.1439-0485.1993.tb00364.x

Swalla BJ (2004) Procurement and culture of ascidian embryos. *Methods in Cell Biology* 74: 115–141, http://dx.doi.org/10.1016/S0091-679X(04)74006-6

Szewzyk U (1991) Relevance of the exopolysaccharide of marine *Pseudomonas sp.* strain S9 for the attachment of *Ciona intestinalis* larvae. *Marine Ecology Progress Series* 75: 259–265, http://dx.doi.org/10.3354/meps075259

Thebault A, Peeler EJ, Murray AG, Brun E, Giovaninni A, Thrush MA (2007) Modelling applications for aquatic animal health. INRA *Productions Animales* 20: 2223–2226

White MT, Griffin JT, Churcher TS, Ferguson NM, Basáñez MG, Ghani AC (2011) Modelling the impact of vector control interventions on *Anopheles gambiae* population dynamics. *Parasites & Vectors* 4: 153, http://dx.doi.org/10.1186/1756-3305-4-153

Wieczorek SK, Todd CD (1997). Inhibition and facilitation of bryozoan and ascidian settlement by natural multi-species biofilms: effects of film age and the roles of active and passive larval attachment. *Marine Biology* 128: 463–473, http://dx.doi.org/10.1007/s002270050113

Yamaguchi M (1975). Growth and reproductive cycles of the marine fouling ascidians *Ciona intestinalis, Styela plicata, Botrylloides violaceus* and *Leptoclinum mitsukurii* at Aburatsubo-Moroiso Inlet (central Japan). *Marine Biology* 29: 253–259, http://dx.doi.org/10.1007/BF00391851

Zapata M, Silva F, Luza Y, Wilkens M, Riquelme C (2007). The inhibitory effect of biofilms produced by wild bacterial isolates to the larval settlement of the fouling ascidia *Ciona intestinalis* and *Pyura praeputialis*. *Electronic Journal of Biotechnology* 10: 149–159, http://dx.doi.org/10.2225/vol10-issue1-fulltext-6

Zega G, De Bernardi F, Groppelli S, Pennati R (2009). Effects of the azole fungicide Imazalil on the development of the ascidian *Ciona intestinalis* (Chordata, Tunicata): Morphological and molecular characterization of the induced phenotype. *Aquatic Toxicology* 91: 255–261, http://dx.doi.org/10.1016/j.aquatox.2008.11.015

Supplementary material is available for this article:

Table S1. Development time for *Ciona intestinalis* at different temperatures;

Table S2. Percentage of fertilization, hatchability, settlement, and metamorphosis of *C. intestinalis* at different temperatures;

Figures S1-S5. The modelled abundance of *C. intestinalis* fitted with the observed temperatures in Georgetown Harbour in 2008.

This material is available as part of online article from:
http://www.reabic.net/journals/mbi/2014/Supplements/MBI_2014_Patanasatienkul_etal_Supplement.pdf